

GRAND for Gaussian Intersymbol Interference Channels

Zhuang Li, Wenyi Zhang, *Senior Member, IEEE*

Abstract—Channel decoding is a challenging task in communication channels exhibiting memory effects. In this work, we apply the recently proposed decoding paradigm of guessing random additive noise decoding (GRAND) to channels with memory, focusing on linear Gaussian intersymbol interference (ISI) channels. For describing error patterns (EPs), we introduce the concept of error burst to account for the memory effect, and define sequence reliability to characterize the likelihood of EP. Based on sequence reliability, we obtain the optimal GRAND algorithm as a generalization of soft GRAND (SGRAND) for linear Gaussian ISI channels, termed SGRAND-ISI, which is equivalent to the maximum-likelihood (ML) decoding algorithm. We then develop order-reliability-bit (ORB) GRAND algorithms based on SGRAND-ISI, to facilitate implementation. In numerical experiments, our proposed algorithms achieve multiple-dB improvements compared to GRAND algorithms which ignore channel memory, and can often attain performance within 0.1–0.2dB of the ML lower bound. We also compare our proposed algorithms with the recently proposed ORBGRAND-Approximate Independence algorithm for handling channel memory, and observe a performance gain of at least 0.5dB at block error rate of 10^{-3} , meanwhile incurring a substantially lower computational complexity.

Index Terms—Channel memory, guessing random additive noise decoding, intersymbol interference, maximum-likelihood decoding, order-reliability-bit, soft decoding.

I. INTRODUCTION

Novel applications such as virtual and augmented reality, vehicle-to-vehicle communication, and machine-type communication have driven the demand for effective ultra-reliable low latency communications (URLLC) solutions [1], [2]. In this context, a new paradigm called guessing random additive noise decoding (GRAND) [3] has been considered as a promising technique for URLLC. In a nutshell, GRAND performs decoding by explicitly identifying the error pattern (EP) introduced during transmission, and it is particularly well-suited to short blocklength and medium-to-high-rate regimes.

While most GRAND-related studies focus on memoryless channels, several extensions have been proposed to cope with channels with memory. GRAND Markov Order (GRAND-MO) [4] targets two-state Markov channels, avoids the commonly adopted interleaver, and shows notable gains over the Berlekamp–Massey decoder [5], [6]. However, GRAND-MO is a hard-decision decoder and thus cannot exploit soft reliability information. Order-reliability-bit (ORB) GRAND-Approximate Independence (ORBGRAND-AI) [7] leverages soft information by partitioning the received sequence into blocks and assuming inter-block independence. Although this avoids interleaving, the inter-block independence approxima-

tion limits its ability to faithfully capture memory effects, resulting in suboptimal performance.

Motivated by these limitations, in this paper, we focus on a canonical and practically important class of memory channels characterized by inter-symbol interference (ISI). We work with first principles and demonstrate how to optimally handle ISI using GRAND without interleaving. Specifically, we introduce the concept of error bursts to characterize the structure and statistics of the EPs induced by ISI channels, and define sequence reliability based on the hard detection sequence [8]. Building on these, we generalize the GRAND criterion in [9] from memoryless channels to ISI channels. By utilizing the exact value of sequence reliability as the decoding metric for generating EPs, maximum-likelihood (ML) decoding can be achieved, and the corresponding decoding algorithm is called soft GRAND-ISI (SGRAND-ISI).

SGRAND-ISI requires on-the-fly computation of sequence reliability, which is costly and hence unfavorable for hardware implementation. To mitigate this, we develop ORBGRAND-ISI, a hardware-friendly suboptimal alternative that preserves the reliability-ordered querying principle while substantially reducing real-time computations. Furthermore, by exploiting the cumulative distribution function (CDF) of sequence reliability, we propose CDF-ORBGRAND-ISI, which provides a notable performance improvement over ORBGRAND-ISI with only a marginal increase in complexity.

We conduct numerical experiments to assess the proposed decoders over both first-order and second-order ISI channels. Simulation results show that, for BCH and polar codes, CDF-ORBGRAND-ISI achieves a gain of at least 2dB even at a block error rate (BLER) of 10^{-1} over ORBGRAND which ignores channel memory. Moreover, relative to ORBGRAND-AI, CDF-ORBGRAND-ISI still provides at least 0.5dB gain at $\text{BLER} = 10^{-3}$ and operates within 0.1–0.2dB of the ML lower bound. We also quantify decoding complexity, demonstrating that CDF-ORBGRAND-ISI is expected to incur significantly less computational costs than ORBGRAND-AI.

The Gaussian ISI channel model serves as the first step towards wireless channels exhibiting significant multipath effects, when the signaling bandwidth exceeds the channel coherence bandwidth [10]. The ISI effect is also ubiquitous in various scenarios, including wired telephone lines and coaxial cables [11], underwater channels [12], optical fiber communications [13], magnetic storage systems [14], and so on. Therefore the methodology established in this work is also of potential relevance in those scenarios.

Equalization has been a standard approach for mitigating ISI. Maximum-likelihood sequence estimation (MLSE) [15] implemented via the Viterbi algorithm [8] achieves optimal sequence detection. But the exponential growth of the computational complexity with the channel memory order motivates

Z. Li and W. Zhang are with Department of Electronic Engineering and Information Science, University of Science and Technology of China, Hefei, China (Email: wenyizha@ustc.edu.cn).

widely used suboptimal equalization techniques such as linear equalization (LE) [16] and decision-feedback equalization (DFE) [17], [18]. For channels with high memory order, an effective solution is channel shortening, in which the receiver first processes the received signal to an impulse response with reduced memory order, and then conducts MLSE [19]–[22]. Even with channel shortening, however, channel decoding is still severely affected by the residual channel memory. Conventional decoder design ignoring channel memory incurs significant performance losses [4], [7]. Turbo equalization [23] iteratively exchanges soft information between equalizer and decoder to improve the performance of decoding, but it meets challenges in URLLC as it possibly incurs substantial complexity, storage, and latency due to its iterative architecture and interleaving/deinterleaving operations.

The remaining part of this paper is organized as follows. Section II establishes the system model and briefly reviews the background of GRAND. Section III analyzes the characteristics of EPs in first-order ISI channels and introduces the corresponding GRAND-ISI algorithm. Section IV extends the solution in Section III to higher-order ISI channels. Section V presents numerical experiments for first- and second-order ISI channels. Section VI concludes this paper.

II. PRELIMINARIES

A. System Model

We consider binary phase shift keying (BPSK) modulation over an ISI channel in which the input-output relationship at the i -th channel use is

$$Y_i = \sum_{l=0}^L h_l W_{i-l} + Z_i, \quad (1)$$

where W_i is the channel input drawn from $\{+1, -1\}$, $Z_i \sim \mathcal{N}(0, \sigma^2)$ is the Gaussian noise, Y_i is the channel output, and $h_0 \cdots, h_L$ are the channel impulse response coefficients, which are assumed to be known to both sides of the transceiver. Without loss of generality, we assume that $\sum_{l=0}^L h_l^2 = 1$, so the signal-to-noise ratio (SNR) is $1/\sigma^2$.

We adopt a codebook \mathcal{C} with code length N and code rate R bits per channel use. The number of messages is given by $M = \lceil 2^{NR} \rceil$. When message $m \in \{1, \dots, M\}$ is transmitted, the corresponding codeword is denoted by $\underline{x}(m) = [x_1(m), \dots, x_N(m)]$, whose elements are drawn from $\{0, 1\}$. The channel input is obtained from the transmitted codeword $\underline{x}(m)$ according to the mapping $W_i = 1 - 2X_i(m)$ for $i = 1, \dots, N$.

Upon receiving a realization \underline{y} of the channel output sequence \underline{Y} , the ML decoding rule is as follows:

$$\begin{aligned} m^* &= \arg \max_{m=1, \dots, M} P_{\underline{Y}|\underline{X}}(\underline{y}|\underline{x}(m)) \\ &= \arg \max_{m=1, \dots, M} \sum_{i=1}^N \ln P_{Y_i|\underline{X}_{i-L:i}}(y_i|\underline{x}_{i-L:i}(m)). \end{aligned} \quad (2)$$

In (2), $\underline{x}_{i-L:i}$ represents x_{i-L}, \dots, x_i . For a given \underline{y} and any sequence $\underline{x} \in \{0, 1\}^N$, whether it is a codeword in \mathcal{C} or not, we define its weight function as

$$\Lambda(\underline{x}, \underline{y}) = \sum_{i=1}^N \ln P_{Y_i|\underline{X}_{i-L:i}}(y_i|\underline{x}_{i-L:i}). \quad (3)$$

In addition, we define the hard detection sequence as

$$\underline{x}^* = \arg \max_{\underline{x} \in \{0, 1\}^N} \Lambda(\underline{x}, \underline{y}), \quad (4)$$

which can be obtained via the Viterbi algorithm.

B. Guessing Random Additive Noise Decoding

GRAND has received widespread attention as a noise-centric decoding paradigm—more precisely, an EP-centric decoding paradigm. The basic idea of GRAND is to sequentially test a series of EPs until a codeword is recovered. When EPs are tested in descending order of likelihood, GRAND realizes ML decoding, even for channels with memory [3]. While GRAND was originally designed for hard-decision channels with binary alphabets, the incorporation of soft reliability information into the decoding process has led to several variants of GRAND. Symbol reliability GRAND [24] indicates the reliability of hard-decision channel output by a single-bit reliability indicator. SGRAND [25] generates EPs based on the magnitudes of log-likelihood ratios (LLRs), thereby fully exploiting soft reliability information and achieving ML decoding. However, the generation of EPs based on exact values of LLRs poses challenges for hardware implementation. ORBGRAND [26] utilizes the relationship of ranking among LLR magnitudes rather than their exact values to generate EPs. This approach enables efficient generation of EPs and hence facilitates hardware implementation [27]–[29]. Notably, ORBGRAND has been shown to achieve an information rate that is very close to channel capacity for commonly used channel models including the additive white Gaussian noise (AWGN) channel [9], [30]. Moreover, rank companding ensures that ORBGRAND is exactly capacity-achieving, and the resulting variant is termed CDF-ORBGRAND [31].

For the system model in Section II-A, GRAND operates as follows. Given the channel output sequence \underline{y} , we form the corresponding hard detection sequence \underline{x}^* . GRAND then generates an ordered list of EPs and, for each EP \underline{e} in this order, conducts a query to test whether $\underline{x}^* \oplus \underline{e}$ is a valid codeword. The procedure terminates once a valid codeword is found, or when the prescribed maximum number of queries is reached. The corresponding pseudo-code is provided in Algorithm 1.

The optimal ordering of EPs, from the most likely to the least likely, is crucial. Unlike memoryless channels wherein EPs can be sorted according to the Hamming weights [24] or the sum of LLR magnitudes [30], for channels with memory, optimally sorting EPs requires further considerations, as will be elaborated in the subsequent sections.

III. GRAND-ISI FOR FIRST-ORDER ISI CHANNELS

In this section, we investigate the properties of EPs in first-order ISI channels ($L = 1$ in (1)) and propose a general form of GRAND, which we term as GRAND-ISI, and its variants.

Algorithm 1 GRAND for an ISI channel

Input: channel output sequence \underline{y} , parity check matrix H , maximum number of queries Q

Output: $\hat{\underline{x}}$ or ABANDON

```

1:  $\underline{x}^* \leftarrow (4)$ 
2:  $q \leftarrow 0$ 
3: while  $q \leq Q$  do
4:    $q = q + 1$ 
5:    $\underline{e} \leftarrow$  next EP
6:   if  $H \cdot (\underline{x}^* \oplus \underline{e})^T = \mathbf{0}$  then
7:     return  $\hat{\underline{x}} = \underline{x}^* \oplus \underline{e}$ 
8:   end if
9: end while
10: return ABANDON

```

A. Error Burst and Sequence Reliability

We frequently consider sets of indices over $\{1, \dots, N\}$, and for convenience, we assume that the elements of any such set are arranged in ascending order. For such a set \mathcal{S} , we denote its smallest and largest elements by $\min(\mathcal{S})$ and $\max(\mathcal{S})$, respectively. Furthermore, we define

$$L_1(\mathcal{S}) = \max\{\min(\mathcal{S}) - 1, 1\}, R_1(\mathcal{S}) = \min\{\max(\mathcal{S}) + 1, N\}.$$

We denote by $f_{\mathcal{S}}(\underline{x})$ the sequence obtained by flipping the bits of \underline{x} at the positions specified by \mathcal{S} . The i -th element of this sequence is denoted by $[f_{\mathcal{S}}(\underline{x})]_i$, and the subsequence from index i to j is denoted by $[f_{\mathcal{S}}(\underline{x})]_{i:j}$.

When transmitting \underline{x} , the corresponding target EP is given by $\underline{e} = \underline{x}^* \oplus \underline{x}$, where \underline{x}^* is given by (4). We denote the corresponding index set $\mathcal{I}(\underline{e}) = \{i : e_i = 1\}$.

Definition 1: For an EP \underline{e} with index set $\mathcal{I}(\underline{e})$, we call the following unique partitioning of $\mathcal{I}(\underline{e})$, $\{\mathcal{I}_i : i = 1, \dots, \zeta(\mathcal{I}(\underline{e}))\}$, the error bursts of \underline{e} :

- The sets $\{\mathcal{I}_i : i = 1, \dots, \zeta(\mathcal{I}(\underline{e}))\}$ form a partitioning of $\mathcal{I}(\underline{e})$, i.e.,

$$\bigcup_{i=1}^{\zeta(\mathcal{I}(\underline{e}))} \mathcal{I}_i = \mathcal{I}(\underline{e}) \quad \text{and} \quad \mathcal{I}_i \cap \mathcal{I}_j = \emptyset \quad \forall i \neq j.$$

- For each \mathcal{I}_i , its elements are consecutive integers.
- For any two \mathcal{I}_i and \mathcal{I}_j , $i \neq j$, there exists at least one integer separating them, i.e., $\max(\mathcal{I}_i) < k < \min(\mathcal{I}_j)$ for some integer k .

Example 1: Suppose that the transmitted codeword is $\underline{x} = 0000000$, and the hard detection sequence is $\underline{x}^* = 0100111$. Therefore, $\underline{e} = \underline{x}^* \oplus \underline{x} = 0100111$, $\mathcal{I}(\underline{e}) = \{2, 5, 6, 7\}$, $\mathcal{I}_1 = \{2\}$, $\mathcal{I}_2 = \{5, 6, 7\}$, and $\zeta(\mathcal{I}(\underline{e})) = 2$.

Therefore, from the definition, when the code length is N , there are in total $\frac{N(N+1)}{2}$ possible error bursts, ranging from

size 1 to N . We denote all these possible error bursts as

$$\text{IND} = \left\{ \underbrace{\{1\}, \dots, \{N\}}_{\text{size 1}}, \underbrace{\{1, 2\}, \dots, \{N-1, N\}}_{\text{size 2}}, \dots, \underbrace{\{1, \dots, N\}}_{\text{size } N} \right\}.$$

Definition 2: Given a channel output sequence \underline{y} and its hard detection sequence \underline{x}^* , for a set $\mathcal{S} \subseteq \{1, \dots, N\}$, its sequence reliability is defined as:

$$\text{Rel}(\mathcal{S}) = \Lambda(\underline{x}^*, \underline{y}) - \Lambda(f_{\mathcal{S}}(\underline{x}^*), \underline{y}). \quad (5)$$

B. General Form of GRAND-ISI

In general, a GRAND-ISI algorithm tests EPs against the hard detection sequence, and we can describe its operation as follows:

- Enumerate all subsets of $\{1, \dots, N\}$ and sort them in ascending order based on their reliability sums

$$\text{RS} \triangleq \left\{ \sum_{t=1}^{\zeta(\mathcal{I})} \gamma(\underline{y}, \mathcal{I}_t) : \mathcal{I} \subseteq \{1, \dots, N\} \right\}, \quad (6)$$

where each subset \mathcal{I} corresponds to an EP consisting of $\zeta(\mathcal{I})$ error bursts and \mathcal{I}_t denotes the t -th error burst of \mathcal{I} , as specified by Definition 1. We adopt a general non-negative function $\gamma(\underline{y}, \mathcal{I}_t)$ to quantify the reliability information of the channel output sequence \underline{y} at the indices specified by \mathcal{I}_t ; concrete examples will be described in the sequel.

- Following the order specified by sorting RS in the preceding stage, for each subset \mathcal{I} , flip the corresponding bits in the hard detection sequence \underline{x}^* to obtain $f_{\mathcal{I}}(\underline{x}^*)$.
- Test whether $f_{\mathcal{I}}(\underline{x}^*)$ is a codeword. If so, stop and declare it as the decoding outcome; otherwise, proceed to the next subset and repeat the testing procedure unless the maximum number of queries Q is reached.

In fact, if Q is equal to the size of RS, the GRAND-ISI algorithm can be equivalently represented as

$$\hat{m} = \arg \min_{m=1, \dots, M} \sum_{t=1}^{\zeta(\mathcal{I}(\underline{e}(m)))} \gamma(\underline{y}, \mathcal{I}_t(\underline{e}(m))). \quad (7)$$

Different choices of γ lead to different sorting outcomes of EPs, thereby resulting in different GRAND-ISI algorithms. This is a natural generalization of the unified representation of GRAND algorithms developed in [9]. Here we list some examples as follows:

- When $\gamma(\underline{y}, \mathcal{I}_t) = \text{Rel}(\mathcal{I}_t)$ as introduced in Definition 2, (7) is called SGRAND-ISI, since it is the extension of SGRAND [25] for ISI channels. See Section III-D for details.
- When $\gamma(\underline{y}, \mathcal{I}_t) = r(\mathcal{I}_t)$, where $r(\mathcal{I}_t)$ is the rank of $\text{Rel}(\mathcal{I}_t)$ among the sequence reliabilities of all error

bursts in IND, from 1 (the smallest) to $\frac{N(N+1)}{2}$ (the largest), (7) is called ORBGRAND-ISI as an extension of ORBGRAND [26] for ISI channels.

- When $\gamma(\underline{y}, \mathcal{I}_t) = \Psi^{-1}\left(\frac{r(\mathcal{I}_t)}{N(N+1)/2+1}\right)$, where $\Psi(\cdot)$ is the CDF of the sequence reliabilities of all error bursts, (7) is CDF-ORBGRAND-ISI. The idea underlying CDF-ORBGRAND can be traced back to [26]. Moreover, [31] establishes that, over memoryless binary-input channels, CDF-ORBGRAND is exactly capacity-achieving.

Similar to the fact that for memoryless channels SGRAND is equivalent to ML decoding, we have the following result regarding SGRAND-ISI.

Theorem 1: When the maximum number of queries Q is equal to the size of RS, SGRAND-ISI is equivalent to ML decoding.

Proof: See Appendix VII-A. ■

C. Properties of Sequence Reliability

In this subsection, we present several properties of sequence reliability, and they will be useful for calculating decoding metrics when implementing GRAND-ISI algorithms.

Lemma 1: For any subset $\mathcal{W} \subseteq \{1, \dots, N\}$, if \mathcal{W} satisfies: $\mathcal{W} = \mathcal{W}_1 \cup \mathcal{W}_2$, $\mathcal{W}_1 \cap \mathcal{W}_2 = \emptyset$, and $\min(\mathcal{W}_2) - \max(\mathcal{W}_1) > 1$, then \mathcal{W} is called decomposable and we have

$$\text{Rel}(\mathcal{W}) = \text{Rel}(\mathcal{W}_1) + \text{Rel}(\mathcal{W}_2). \quad (8)$$

Proof: See Appendix VII-B. ■

Lemma 2: If a subset $\mathcal{W} \subseteq \{1, \dots, N\}$ satisfies $\mathcal{W} = \{a, a+1, \dots, a+|\mathcal{W}|-1\}$, $a \in \mathcal{N}^+$, then \mathcal{W} is called non-decomposable and we have

$$\begin{aligned} \text{Rel}(\mathcal{W}) &= \sum_{i=a}^{a+|\mathcal{W}|-1} \text{Rel}(\{i\}) \\ &= \sum_{i=a}^{a+|\mathcal{W}|-2} \left(\text{Rel}(\{i, i+1\}) - \text{Rel}(\{i\}) - \text{Rel}(\{i+1\}) \right). \end{aligned} \quad (9)$$

Proof: See Appendix VII-C. ■

Lemma 3: In Lemma 2, $\text{Rel}(\{i, i+1\}) - \text{Rel}(\{i\}) - \text{Rel}(\{i+1\})$ can be uniquely determined by the hard detection sequence \underline{x}^* according to

$$\begin{aligned} &\text{Rel}(\{i, i+1\}) - \text{Rel}(\{i\}) - \text{Rel}(\{i+1\}) \\ &= \frac{4h_0h_1}{\sigma^2} [2 \times \mathbf{1}(x_i^* = x_{i+1}^*) - 1]. \end{aligned} \quad (10)$$

Proof: See Appendix VII-D. ■

D. SGRAND-ISI

If the hard detection sequence \underline{x}^* is a codeword, SGRAND-ISI immediately outputs it as the decoding result. Otherwise, it needs to compute the sequence reliabilities for all the $\frac{N(N+1)}{2}$ error bursts in IND. Facilitated by lemmas presented in the previous subsection, this computation can be significantly simplified as follows:

Step 1: Compute the sequence reliabilities for all error bursts of size 1;

Step 2: Iteratively compute the sequence reliabilities for longer error bursts using Lemmas 2 and 3.

After obtaining the sequence reliabilities for all error bursts, we need to perform SGRAND-ISI according to (7). Candidate EPs can be generated by the heap algorithm in [25] or the parallel algorithm in [32]. In each iteration, such algorithms simply choose several error bursts from IND to produce a candidate EP. However, in light of Definition 1, for such chosen error bursts to assemble a valid EP, they should not overlap, and any two of them should be separated by at least one position. Any candidate EP not satisfying these criteria is expurgated, and only the surviving ones lead to valid EPs to be tested by parity-check matrix verification.

Example 2: Consider a first-order ISI channel and block-length $N = 4$. Let $h_0 = \sqrt{0.9}$, $h_1 = \sqrt{0.1}$, the noise variance be $\sigma^2 = 1$, so $\frac{4h_0h_1}{\sigma^2} = 1.2$. Suppose that we obtain a realization where the received vector is

$$\underline{y} = [0.63, 0.87, 0.8, -1.77].$$

We obtain $\underline{x}^* = 0001$ and the sequence reliabilities for all error bursts of size 1 are:

$$\begin{aligned} \text{Rel}(\{1\}) &= 1.14, \text{Rel}(\{2\}) = 0.95, \text{Rel}(\{3\}) = 0.39, \\ \text{Rel}(\{4\}) &= 3.96, \end{aligned}$$

Based on Lemmas 2 and 3, the sequence reliabilities of all error bursts can be evaluated,

$$\begin{aligned} \text{Rel}(\{1, 2\}) &= 3.29, \text{Rel}(\{2, 3\}) = 2.54, \text{Rel}(\{3, 4\}) = 3.15, \\ \text{Rel}(\{1, 2, 3\}) &= 4.88, \text{Rel}(\{2, 3, 4\}) = 5.3, \\ \text{Rel}(\{1, 2, 3, 4\}) &= 7.64. \end{aligned}$$

With these, candidate EPs can be sequentially generated. Each candidate EP is represented as a length- $\frac{N(N+1)}{2}$ binary vector whose positions correspond to the elements in IND, and only those chosen error bursts have their corresponding positions marked as one. As discussed, an additional check is invoked to expurgate those invalid candidate EPs, i.e., those assembled by overlapping or consecutive error bursts. For example, the candidate EP 1001000000 consists of error bursts $\{3\}$ and $\{2, 3\}$, but since these two error bursts overlap, this candidate EP is invalid and immediately expurgated; the candidate EP 0000011000 consists of error bursts $\{1, 2\}$ and $\{4\}$, which satisfy the conditions in Definition 1, and hence this corresponds to a valid EP 1101, which is then used for subsequent parity-check matrix verification.

The pseudocode of SGRAND-ISI is presented in Algorithm 2. Therein, in addition to the maximum number of queries for parity-check matrix verification Q , we also introduce the maximum number of candidate EPs Q_1 . In light of the description in the preceding paragraph, we generate at most Q_1 candidate EPs, regardless of whether it corresponds to a valid EP or not, and we allow at most Q valid EPs for parity-check matrix verification.

E. ORBGRAND-ISI

While SGRAND-ISI has the optimal performance as shown in Theorem 1, it requires the exact value of sequence reliability to generate EPs, hindering efficient hardware implementation.

Algorithm 2 SGRAND-ISI for ISI channels

Input: \underline{x}^* , H , Rel , IND , Q , Q_1
Output: $\hat{\underline{x}}$ or ABANDON
 1: $\underline{r} \leftarrow \text{sort}(\text{Rel})$
 2: $q \leftarrow 0, p \leftarrow 0, \mathcal{S} \leftarrow \{0\}$
 3: **while** $q \leq Q_1$ **do**
 4: candidate EP $\underline{v} \leftarrow \arg \min_{\underline{v} \in \mathcal{S}} \underline{v} \cdot \text{Rel}$
 5: $\mathcal{S} = \mathcal{S} \setminus \{\underline{v}\}, q = q + 1$
 6: $\underline{t} \leftarrow \text{check validity for } \underline{v}$
 7: **if** $\underline{t} = 1$ **then**
 8: $p = p + 1$
 9: $\underline{e} \leftarrow (\underline{v}, \text{IND})$
 10: **if** $H \cdot (\underline{x}^* \oplus \underline{e})^T = 0$ **then**
 11: **return** $\hat{\underline{x}} = \underline{x}^* \oplus \underline{e}$
 12: **end if**
 13: **if** $p = Q$ **then**
 14: **return** ABANDON
 15: **end if**
 16: **end if**
 17: **if** $\underline{v} = 0$ **then**
 18: $i_* = 0$
 19: **else**
 20: $i_* = \max \{i : v_{r_i} \neq 0\}$
 21: **end if**
 22: **if** $i_* < \text{length}(\underline{r})$ **then**
 23: $v_{r_{(i_*+1)}} = 1, \mathcal{S} = \mathcal{S} \cup \{\underline{v}\}$
 24: **if** $i_* > 0$ **then**
 25: $v_{r_{i_*}} = 0, \mathcal{S} = \mathcal{S} \cup \{\underline{v}\}$
 26: **end if**
 27: **end if**
 28: **end while**
 29: **return** ABANDON

Leveraging the idea of ORBGRAND [26], we can analogously devise the ORBGRAND-ISI algorithm, with $\gamma(\underline{y}, \mathcal{I}_t) = r(\mathcal{I}_t)$, the rank of $\text{Rel}(\mathcal{I}_t)$ among the sequence reliabilities of all error bursts in IND , from 1 (the smallest) to $\frac{N(N+1)}{2}$ (the largest), to facilitate hardware implementation.

In order to alleviate the mismatch between sequence reliability and its ranking, we also consider a modification of ORBGRAND-ISI, termed CDF-ORBGRAND-ISI, which essentially leverages a companding technique to transform the rank of each sequence reliability according to the inverse CDF of sequence reliability, with $\gamma(\underline{y}, \mathcal{I}_t) = \Psi^{-1}\left(\frac{r(\mathcal{I}_t)}{N(N+1)/2+1}\right)$. In Fig. 1 we present the CDFs of sequence reliability at different SNRs in a first-order ISI channel. Compared to ORBGRAND-ISI, the reliability information used by CDF-ORBGRAND-ISI is more aligned with the exact sequence reliability used by SGRAND-ISI, and our numerical experiments in Section V show that this leads to evident performance improvements.

IV. GRAND-ISI FOR HIGHER-ORDER ISI CHANNELS

In the previous section, we have studied GRAND-ISI for first-order ISI channels, and in this section we extend the analysis to more general L -th-order ISI channels. In this case,

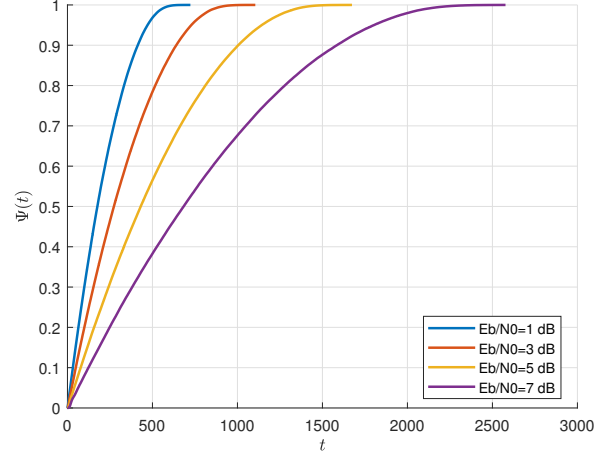


Fig. 1. CDFs of sequence reliability in the first-order ISI channel for CA-Polar(128,114+6) with $(h_0, h_1) = (\sqrt{0.9}, \sqrt{0.1})$, where the CRC-6 generator polynomial is $g(x) = x^6 + x + 1$.

the definition of the smallest and largest elements for a set remains the same. For convenience of writing, we also define $L_L(\mathcal{S}) = \max(\min(\mathcal{S}) - L, 1)$, $R_L(\mathcal{S}) = \min(\max(\mathcal{S}) + L, N)$. The definition of error burst is generalized as follows:

Definition 3: For an EP \underline{e} with index set $\mathcal{I}(\underline{e})$, we call the following unique partitioning of $\mathcal{I}(\underline{e})$, $\{\mathcal{I}_i : i = 1, \dots, \zeta(\mathcal{I}(\underline{e}))\}$, the error bursts of \underline{e} :

- The sets \mathcal{I}_i form a partitioning of $\mathcal{I}(\underline{e}(m))$, i.e.,

$$\bigcup_{i=1}^{\zeta(\mathcal{I}(\underline{e}))} \mathcal{I}_i = \mathcal{I}(\underline{e}) \quad \text{and} \quad \mathcal{I}_i \cap \mathcal{I}_j = \emptyset \quad \forall i \neq j.$$

- For each $\mathcal{I}_i = \{s_1 < s_2 < \dots < s_{|\mathcal{I}_i|}\}$, $s_{j+1} - s_j \leq L$ for $j = 1, \dots, |\mathcal{I}_i| - 1$.
- For any two \mathcal{I}_i and \mathcal{I}_j , $i \neq j$, there exists at least L integers separating them, i.e., $\max(\mathcal{I}_i) + L < \min(\mathcal{I}_j)$.

Example 3: Consider $L = 2$. Suppose that the transmitted codeword is $\underline{x} = 000000$, and the hard detection sequence is $\underline{x}^* = 101001$. Therefore, $\underline{e} = \underline{x}^* \oplus \underline{x} = 101001$, $\mathcal{I}(\underline{e}) = \{1, 3, 6\}$, $\mathcal{I}_1 = \{1, 3\}$, $\mathcal{I}_2 = \{6\}$, and $\zeta(\mathcal{I}(\underline{e})) = 2$.

The definition of sequence reliability and the general form of GRAND-ISI remain the same as those in first-order ISI channels.

A. Properties of Sequence Reliability

The sequence reliability for L -th-order ISI channels is more complicated than that for first-order ISI channels. Nevertheless, we still have the following properties.

Lemma 4: For any subset $\mathcal{W} \subseteq \{1, \dots, N\}$, if \mathcal{W} satisfies: $\mathcal{W} = \mathcal{W}_1 \cup \mathcal{W}_2$, $\mathcal{W}_1 \cap \mathcal{W}_2 = \emptyset$, and $\min(\mathcal{W}_2) - \max(\mathcal{W}_1) > L$, then \mathcal{W} is called decomposable and we have

$$\text{Rel}(\mathcal{W}) = \text{Rel}(\mathcal{W}_1) + \text{Rel}(\mathcal{W}_2). \quad (11)$$

Proof: See Appendix VII-E. ■

For first-order ISI channels in Section III, \mathcal{W} is called non-decomposable if it satisfies $\mathcal{W} = \{a, a + 1, \dots, a + |\mathcal{W}| - 1\}$ for some $a \in \mathcal{N}_+$. The definition of non-decomposability

for higher-order ISI channels remains the same. Furthermore, there arises the partially-decomposable case, as described below:

Lemma 5: For a subset $\mathcal{W} \subseteq \{1, \dots, N\}$, if \mathcal{W} satisfies: $\mathcal{W} = \mathcal{W}_1 \cup \mathcal{W}_2$, $\mathcal{W}_1 \cap \mathcal{W}_2 = \emptyset$, $2 \leq \min(\mathcal{W}_2) - \max(\mathcal{W}_1) \leq L$, then \mathcal{W} is called partially-decomposable and satisfies:

$$\begin{aligned} & \text{Rel}(\mathcal{W}) \\ &= \text{Rel}(\mathcal{W}_1) + \text{Rel}(\mathcal{W}_2) \\ &+ \sum_{i=\min(\mathcal{W}_2)}^{R_L(\mathcal{W}_1)} \left(\ln \frac{P_{Y_i|\underline{x}_{i-L:i}}(y_i|[f_{\mathcal{W}_1}(\underline{x}^*)]_{i-L:i})}{P_{Y_i|\underline{x}_{i-L:i}}(y_i|[\underline{x}_{i-L:i}^*])} \right. \\ &\left. + \ln \frac{P_{Y_i|\underline{x}_{i-L:i}}(y_i|[f_{\mathcal{W}_2}(\underline{x}^*)]_{i-L:i})}{P_{Y_i|\underline{x}_{i-L:i}}(y_i|[f_{\mathcal{W}}(\underline{x}^*)]_{i-L:i})} \right). \end{aligned} \quad (12)$$

Proof: See Appendix VII-F. \blacksquare

Example 4: Consider a second-order ISI channel with $h_0 = \sqrt{0.8}$, $h_1 = \sqrt{0.15}$, $h_2 = \sqrt{0.05}$, and $\sigma^2 = 1$. Let code length be $N = 4$. Suppose that we obtain a realization where the received vector is

$$\underline{y} = [0.14, -0.28, 0.44, 0.66].$$

We obtain $\underline{x}^* = 1001$ and the sequence reliabilities are:

$$\begin{aligned} & \text{Rel}(\{1\}) = 0.70, \text{Rel}(\{2\}) = 2.00, \text{Rel}(\{3\}) = 1.08, \\ & \text{Rel}(\{4\}) = 0.89, \\ & \text{Rel}(\{1, 2\}) = 0.98, \text{Rel}(\{1, 3\}) = 2.58, \text{Rel}(\{1, 4\}) = 1.59, \\ & \text{Rel}(\{2, 3\}) = 1.35, \text{Rel}(\{2, 4\}) = 2.09, \text{Rel}(\{3, 4\}) = 3.35, \\ & \text{Rel}(\{1, 2, 3\}) = 1.12, \text{Rel}(\{1, 2, 4\}) = 1.07, \\ & \text{Rel}(\{1, 3, 4\}) = 4.86, \text{Rel}(\{2, 3, 4\}) = 2.83, \\ & \text{Rel}(\{1, 2, 3, 4\}) = 2.6. \end{aligned}$$

Now take the set $\mathcal{W}_p = \{1, 3\}$ and $\mathcal{W}_d = \mathcal{W}_1 \cup \mathcal{W}_2$ with $\mathcal{W}_1 = \{1\}$ and $\mathcal{W}_2 = \{3\}$. Then \mathcal{W}_p is partially-decomposable, and we have

$$\text{Rel}_{\mathcal{W}_p} = \text{Rel}(\{1, 3\}) = 2.58,$$

while

$$\text{Rel}_{\mathcal{W}_1} + \text{Rel}_{\mathcal{W}_2} = \text{Rel}(\{1\}) + \text{Rel}(\{3\}) = 1.78.$$

In contrast, for $\mathcal{W}_d = \{1, 4\}$ and $\mathcal{W}_d = \mathcal{W}_1 \cup \mathcal{W}_3$ with $\mathcal{W}_3 = \{4\}$, \mathcal{W}_d is decomposable, and we have

$$\text{Rel}_{\mathcal{W}_d} = \text{Rel}(\{1, 4\}) = 1.59 = \text{Rel}_{\mathcal{W}_1} + \text{Rel}_{\mathcal{W}_3}.$$

In the case of first-order ISI channels, the properties of sequence reliability as described by the lemmas in Section III-C enable iterative computation of sequence reliabilities of error bursts. For higher-order ISI channels, however, the properties are less useful than those in the first-order case, and it may sometimes be more convenient to compute sequence reliabilities of error bursts directly from Definition 2.

B. Approximation Strategy

As shown in the previous subsection, for higher-order ISI channels, error bursts are classified into two types: non-decomposable and partially-decomposable. For non-decomposable error bursts, $N + 1 - i$ of them have size i , for $i = 1, \dots, N$, resulting in a total of $\frac{N(N+1)}{2}$ error bursts. The total number of partially-decomposable error bursts, however, becomes prohibitively large, making exhaustive enumeration impractical. To address this difficulty, approximations are employed by restricting the consideration to error bursts of specific, usually small, sizes. Numerical experiments in the next section demonstrate that such an approximation strategy for SGRAND-ISI incurs little performance degradation when partially-decomposable error bursts are judiciously included for evaluation. The following example provides an illustration in second-order ISI channels.

Example 5: In second-order ISI channels, there are $(N - 2)$ partially-decomposable error bursts of size 2, and $(N - 4) + 2(N - 3)$ partially-decomposable error bursts of size 3 (assuming $N \geq 4$). For reducing the computational complexity, partially-decomposable error bursts of sizes larger than 3 are not considered. After computing the sequence reliabilities for non-decomposable and partially-decomposable error bursts, the subsequent operations of decoding are essentially the same as those in first-order ISI channels.

Correspondingly, when only the ranking of sequence reliability, rather than its exact value, is used to generate EPs, we obtain ORBGRAND-ISI and CDF-ORBGRAND-ISI algorithms, similar to the description in Section III-E.

V. NUMERICAL EXPERIMENTS

In this section, we present results of numerical experiments. We mainly study two codes: CA-Polar(128,114+6) with CRC-6 generator polynomial $g(x) = x^6 + x + 1$ and BCH(127,113) for illustration.

A. First-order ISI Channels

First, we present numerical experimental results for first-order ISI channels.

For comparison, we study the following decoding algorithms:

- SGRAND-ISI;
 - ORBGRAND-ISI;
 - 2line-ORBGRAND-ISI which adopts a piecewise linear approximation of CDF as in [26] to enhance ORBGRAND-ISI;
 - CDF-ORBGRAND-ISI.
 - ORBGRAND-AI in [7].¹
- For all the above five decoding algorithms we set $Q = 1 \times 10^4$ and $Q_1 = 1.5 \times 10^5$.
- ORBGRAND without considering channel memory, with $Q = 1.5 \times 10^5$.

We also include a baseline of genie-aided ML lower bound.

¹To facilitate a fair comparison, two query limits are also imposed in the implementation of ORBGRAND-AI: the maximum number of candidate EPs Q_1 , and the maximum number of valid EPs Q used for parity-check matrix verification.

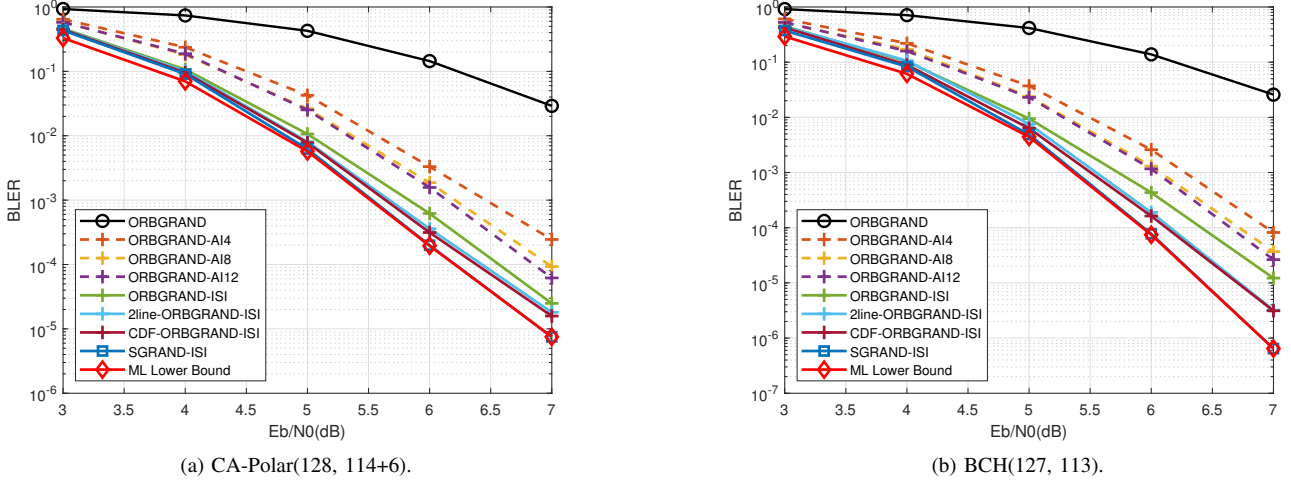


Fig. 2. Performance in the first-order ISI channel with $h_0 = \sqrt{0.9}$ and $h_1 = \sqrt{0.1}$.

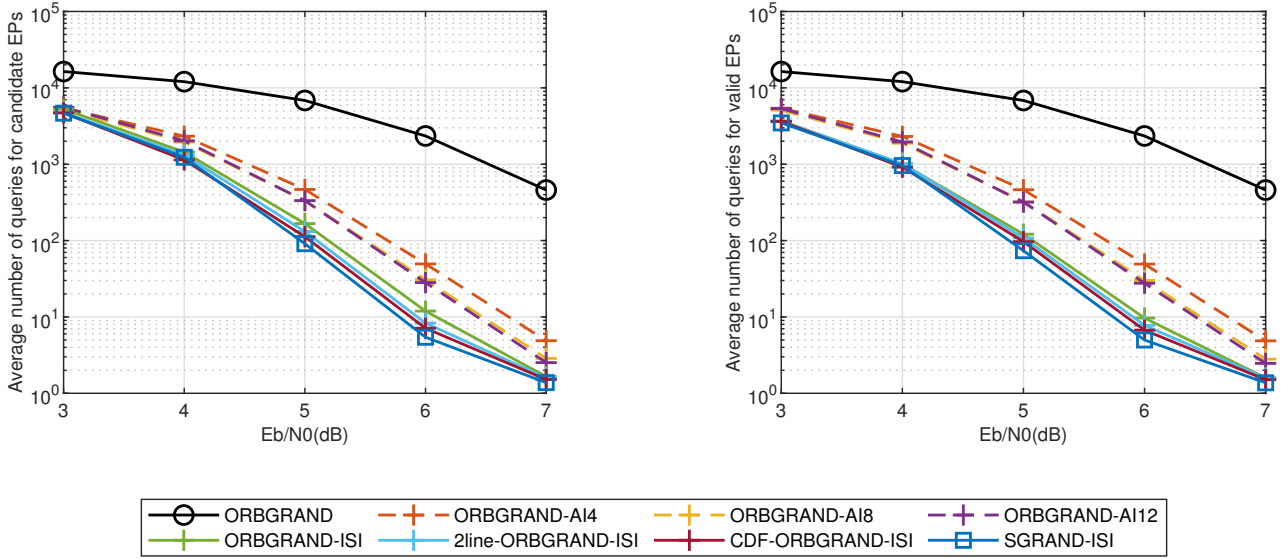


Fig. 3. Average number of queries in first-order ISI channel with $h_0 = \sqrt{0.9}$, $h_1 = \sqrt{0.1}$ for CA-Polar(128, 114+6).

For $h_0 = \sqrt{0.9}$, $h_1 = \sqrt{0.1}$, the results for CA-Polar(128, 114+6) and BCH(127, 113) are shown in Fig. 2a and Fig. 2b, respectively. We observe that SGRAND-ISI exhibits negligible deviation from the ML lower bound, with minor discrepancies only noticeable in the low-SNR regime, which is attributed to the truncation for the maximum number of queries; — if the constraints on Q and Q_1 were removed, SGRAND-ISI would achieve the ML decoding performance.

Compared to ORBGRAND ignoring channel memory, CDF-ORBGRAND-ISI achieves nearly a 2dB improvement, even at a BLER of 10^{-1} . Relative to ORBGRAND-AI12, CDF-ORBGRAND-ISI still provides a 0.6dB improvement at a BLER of 10^{-3} , narrowing the gap to the ML lower bound to just 0.1dB. CDF-ORBGRAND-ISI and 2line-ORBGRAND-ISI achieve very similar performance, both providing a 0.2dB

performance gain over ORBGRAND-ISI at a BLER of 10^{-3} .

Moreover, we present the average number of queries for candidate EPs and the average number of queries for valid EPs in Fig. 3 and Fig. 4. Among all algorithms, SGRAND-ISI incurs the fewest queries, and CDF-ORBGRAND-ISI the second fewest. Although SGRAND-ISI requires fewer queries than CDF-ORBGRAND-ISI, it depends on exact values of sequence reliabilities to dynamically generate EPs, which in turn leads to the highest computational complexity in implementation.

As ISI strengthens, for instance, when $h_0 = \sqrt{0.6}$, $h_1 = \sqrt{0.4}$, the decoding performance of various algorithms is presented in Fig. 5. We observe that ORBGRAND ignoring channel memory suffers from severe performance degradation, with BLER approaching 100%. In contrast, our proposed

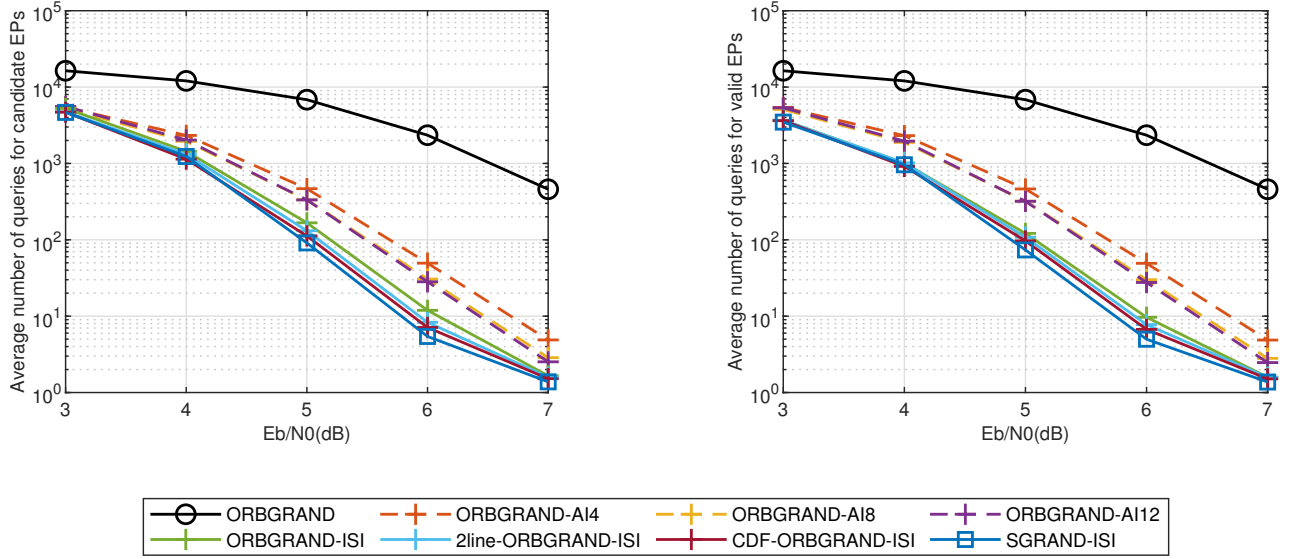


Fig. 4. Average number of queries in first-order ISI channel with $h_0 = \sqrt{0.9}$, $h_1 = \sqrt{0.1}$ for BCH(127, 113).

algorithms sustain robust decoding performance and yield substantial gains over ORBGRAND-AI. Specifically, at a BLER of 10^{-3} , CDF-ORBGRAND-ISI achieves a 1dB improvement compared to ORBGRAND-AI12, remaining within 0.15dB of the ML lower bound.

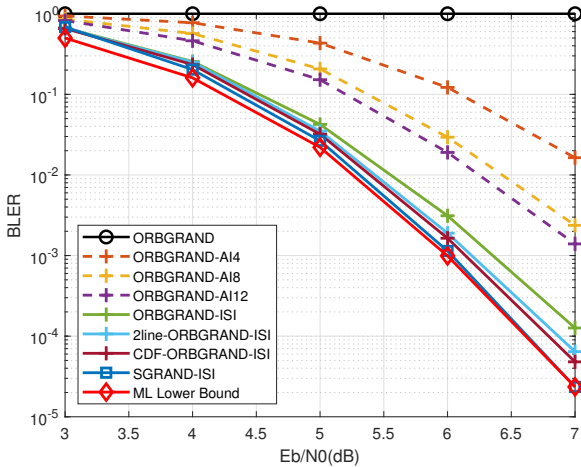


Fig. 5. Performance in first-order ISI channel with $h_0 = \sqrt{0.6}$, $h_1 = \sqrt{0.4}$ for BCH(127, 113).

The notably poor performance of ORBGRAND ignoring channel memory can be explained by inspecting the average logistic weight of target EPs, which reflects the average number of queries required for successful decoding. In Fig. 6, we observe that within the selected SNR range, for $h_0 = 1$ (i.e., memoryless channel without ISI), the average logistic weight of the target EPs is at most 30, corresponding to about 2000 required number of queries; for $h_0 = \sqrt{0.9}$, the average logistic weight ranges between 10 and 100, which may not be reached by the preset maximum number of queries of

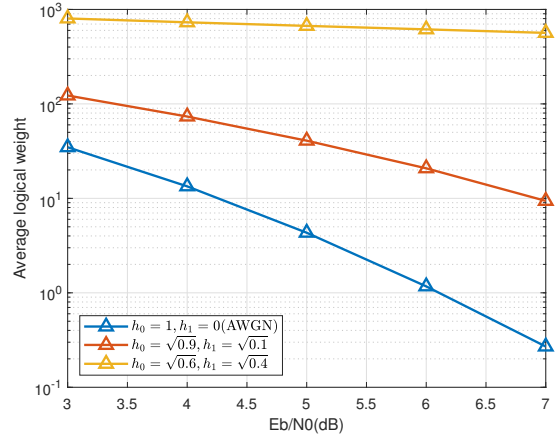


Fig. 6. Average logistic weight of target EP for BCH(127, 113).

$Q = 1.5 \times 10^5$ (corresponding to a logistic weight of 64) for ORBGRAND; for $h_0 = \sqrt{0.6}$, the average logistic weight exceeds 800, far surpassing the capability of ORBGRAND with $Q = 1.5 \times 10^5$, rendering it entirely inoperative in this case.

B. Higher-order ISI Channels

We then consider higher-order ISI channels. Unless stated otherwise, we still use the same choices of the maximum number of queries as those in the previous subsection. We fix the channel coefficients as $h_0 = \sqrt{0.8}$, $h_1 = \sqrt{0.15}$, and $h_2 = \sqrt{0.05}$, corresponding to a channel memory order of $L = 2$.

As discussed in Section IV-B, due to the massive number of possible partially-decomposable error bursts, we only enumerate those of size no greater than g to reduce the computational

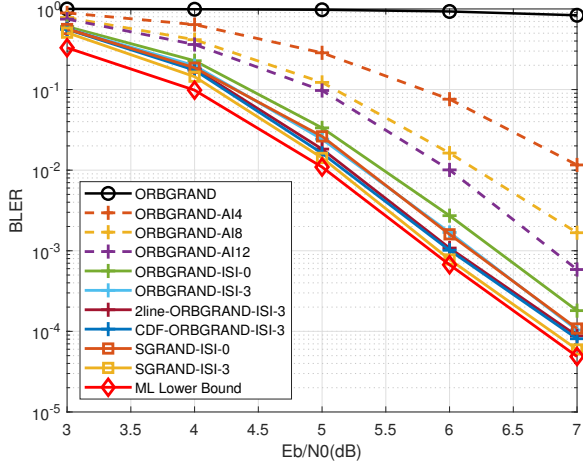


Fig. 7. Performance in second-order ISI channel with $h_0 = \sqrt{0.8}, h_1 = \sqrt{0.15}, h_2 = \sqrt{0.05}$ for CA-Polar(128, 114+6).

complexity. The resulting GRAND algorithms are therefore appended by “- g ” accordingly.

The experimental results for CA-Polar(128,114+6) and BCH(127,113) are illustrated in Fig. 7 and Fig. 8, respectively. We can observe that in this scenario, ORBGRAND, which ignores channel memory, nearly ceases to function, with BLER remaining close to 100% even at high SNR. In addition, we observe that increasing the inclusion of partially-decomposable error bursts improves the performance, narrowing the gap to the ML lower bound; for example, at a BLER of 10^{-3} , SGRAND-ISI-3 achieves a 0.3dB gain over SGRAND-ISI-0, deviating from the ML lower bound of less than 0.1 dB for both CA-Polar(128, 114+6) and BCH(127, 113). Furthermore, CDF-ORBGRAND-ISI-3 offers a 0.8dB gain over ORBGRAND-AI12 while maintaining a 0.2dB gap from the ML lower bound.

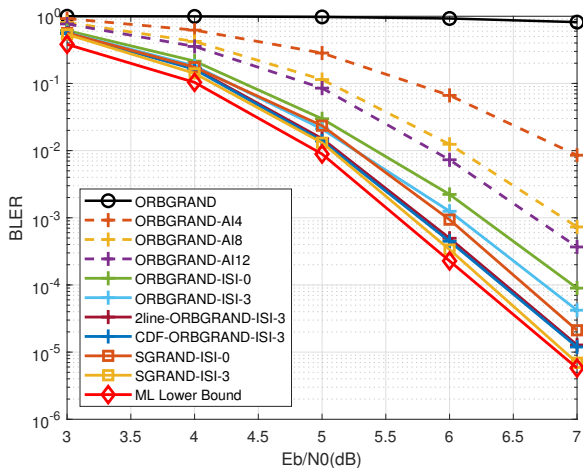


Fig. 8. Performance in second-order ISI channel with $h_0 = \sqrt{0.8}, h_1 = \sqrt{0.15}, h_2 = \sqrt{0.05}$ for BCH(127, 113).

Table I displays statistics of the average number of queries for considered algorithms. For ORBGRAND, each entry de-

TABLE I
AVERAGE NUMBER OF QUERIES FOR BCH(127,113) WITH
 $h_0 = \sqrt{0.8}, h_1 = \sqrt{0.15}, h_2 = \sqrt{0.05}$.

	3dB	5dB	7dB
ORBGRAND	15725.2	15249.8	13056.3
ORBGRAND-AI4	7147.6 / 7112.4	2775.0 / 2758.6	139.7 / 138.9
ORBGRAND-AI8	7286.1 / 7102.3	1338.9 / 1297.6	20.4 / 20.1
ORBGRAND-AI12	7100.7 / 6824.1	1089.5 / 1041.9	10.7 / 10.5
ORBGRAND-ISI-0	7549.3 / 4953.6	514.4 / 331.6	3.6 / 2.9
ORBGRAND-ISI-3	8664.0 / 4681.4	453.8 / 247.8	2.5 / 2.1
2line-ORBGRAND-ISI-3	7060.7 / 4634.8	277.2 / 199.2	1.9 / 1.8
CDF-ORBGRAND-ISI-3	7048.7 / 4608.5	258.0 / 180.5	1.8 / 1.7
SGRAND-ISI-0	6197.2 / 4506.8	336.5 / 250.7	2.0 / 1.9
SGRAND-ISI-3	6618.6 / 4253.8	254.6 / 171.4	1.6 / 1.5

notes the average total number of queries, whereas for the other algorithms, each entry is given in the form of candidate/valid, corresponding to the average numbers of queries for candidate EPs and valid EPs, respectively. We observe that increasing the inclusion of partially-decomposable error bursts reduces the average number of queries in most cases, while for ORBGRAND-ISI and SGRAND-ISI at 3dB the total average number of queries increases. In addition, CDF-ORBGRAND-ISI-3 requires substantially fewer queries than ORBGRAND-AI and ORBGRAND-ISI-3. On the other hand, although SGRAND-ISI-3 yields fewer queries than CDF-ORBGRAND-ISI-3, nevertheless, its real-time computational demands result in the highest complexity of implementation, as pointed out earlier.

C. Complexity Analysis

In this subsection, we provide an analysis of algorithm complexity. The procedure involved in ORBGRAND-ISI can be broken down into three main steps: (1) acquiring the hard detection sequence, (2) calculating the sequence reliability for each error burst, and (3) generating and testing the burst patterns. Compared with ORBGRAND-ISI, CDF-ORBGRAND-ISI and 2line-ORBGRAND-ISI only require additional table-lookup according to Fig. 1, with rather marginal additional cost.

In the first step, the receiver employs the Viterbi algorithm to obtain the hard detection sequence, with a complexity of $\mathcal{O}(N \cdot 2^L)$, where N is code length and L is ISI channel order. If the hard detection sequence is already a codeword, it is immediately declared as decoding result; otherwise, ORBGRAND-ISI proceeds to calculate and sort the sequence reliabilities for error bursts. The complexity of this second step is determined by the total number of sequence reliability calculations required, denoted as tot , which can be calculated as follows:

$$F(i) = 1 + \sum_{j=\max\{1, i-L\}}^{i-1} F(j), \quad i = 1, 2, \dots, N,$$

$$\text{tot} = \sum_{i=1}^N F(i). \quad (13)$$

TABLE II
COMPARISON OF COMPLEXITY BETWEEN ORBGRAND-AI AND
ORBGRAND-ISI AT $E_b/N_0 = 4$ dB IN FIG. 2A.

	Step 1	Step 2	Step 3
ORBGRAND-AI4	$\mathcal{O}(N \cdot 2^L)$	480	2328.5 / 2311.2
ORBGRAND-AI8	$\mathcal{O}(N \cdot 2^L)$	4080	1948.6 / 1885.2
ORBGRAND-AI12	$\mathcal{O}(N \cdot 2^L)$	41205	2024.8 / 1958.3
ORBGRAND-ISI	$\mathcal{O}(N \cdot 2^L)$	8256	1440.0 / 1007.1
2line-ORBGRAND-ISI	$\mathcal{O}(N \cdot 2^L)$	8256	1320.6 / 1015.8
CDF-ORBGRAND-ISI	$\mathcal{O}(N \cdot 2^L)$	8256	1138.0 / 914.7

Taking $L = 2$ as an example, we can use the above recursive relationship to get

$$\text{tot} = \frac{(2\varphi + 1)\varphi^{N+1} - (2\psi + 1)\psi^{N+1}}{\sqrt{5}} - N - 3, \quad (14)$$

where $\varphi \triangleq \frac{1+\sqrt{5}}{2}$ and $\psi \triangleq \frac{1-\sqrt{5}}{2}$. So tot grows exponentially with N , and it is necessary to employ the approximation strategy described in Section IV-B to alleviate the computational burden.

The computational complexity of the third step can be quantified by the number of queries, as displayed in Table I; see also Fig. 3 and Fig. 4.

For ORBGRAND-AI, as described in [7], its procedure can also be divided into the same three steps. Therefore, we can compare its complexity with ours. Taking $E_b/N_0 = 4$ dB in Fig. 2a as an example, the results are summarized in Table II, where *Step 1* refers to the complexity of the Viterbi algorithm (assuming $L \leq$ block length), *Step 2* denotes the number of sequence reliabilities to be computed (or reliabilities in ORBGRAND-AI), and *Step 3* reports the average number of queries (each entry is given in the form of candidate/valid, corresponding to the average numbers of queries for candidate EPs and valid EPs, respectively). We observe that ORBGRAND-ISI, 2line-CDF-ORBGRAND-ISI, and CDF-ORBGRAND-ISI incur similar computational complexity. Compared to ORBGRAND-AI12, the number of computed sequence reliabilities is reduced by about a factor of five, and the corresponding number of queries is also reduced accordingly.

VI. CONCLUSION

In this paper, we exploit the recently proposed GRAND paradigm to optimally handle channel memory. To describe the structure and statistics of EPs arising from ISI, we formulate an error burst representation and, on this basis, define sequence reliability. Based on this, we propose SGRAND-ISI, which can achieve ML decoding, and ORBGRAND-ISI, which is suitable for hardware implement. Numerical results show that, relative to conventional decoders that ignore channel memory, the proposed schemes deliver multi-dB gains and operate within 0.1–0.2dB of the ML lower bound. Moreover, compared with ORBGRAND-AI, which also targets channels with memory, our approach achieves an additional 0.6–1dB gain while requiring substantially lower decoding complexity.

It was shown in [31] that CDF-ORBGRAND is exactly capacity-achieving for general memoryless binary-input chan-

nels. Whether its ISI extension, CDF-ORBGRAND-ISI, remains capacity-achieving is still unaddressed. Future works include characterizing the achievable rates of ORBGRAND-ISI and CDF-ORBGRAND-ISI for channels with memory, and to optimize the approximation strategy of SGRAND-ISI for higher-order ISI channels to further reduce its performance loss.

VII. APPENDICES

A. Proof of Theorem 1

Denote $\mathcal{B}_t(m) = \mathcal{I}_t(\underline{e}(m)) \cup \{\mathbf{R}_1(\mathcal{I}_t(\underline{e}(m)))\}$ for $t = 1, \dots, \zeta(\mathcal{I}(\underline{e}(m)))$ and $\mathcal{B}(m) = \mathcal{B}_1(m) \cup \mathcal{B}_2(m) \dots \cup \mathcal{B}_{\zeta(\mathcal{I}(\underline{e}(m)))}(m)$. Based on the definition of (5), we have

$$\begin{aligned} & \zeta(\mathcal{I}(\underline{e}(m))) \\ & \sum_{t=1}^{\zeta(\mathcal{I}(\underline{e}(m)))} \text{Rel}(\mathcal{I}_t(\underline{e}(m))) \\ &= \sum_{t=1}^{\zeta(\mathcal{I}(\underline{e}(m)))} \sum_{i=\min(\mathcal{I}_t(\underline{e}(m)))}^{\mathbf{R}_1(\mathcal{I}_t(\underline{e}(m)))} \ln \frac{P_{Y_i|\mathcal{X}_{i-1:i}}(y_i|\underline{x}_{i-1:i}^*)}{P_{Y_i|\mathcal{X}_{i-1:i}}(y_i|[f_{\mathcal{I}_t}(\underline{x}^*)]_{i-1:i})} \\ &= \sum_{t=1}^{\zeta(\mathcal{I}(\underline{e}(m)))} \sum_{i=\min(\mathcal{I}_t(\underline{e}(m)))}^{\mathbf{R}_1(\mathcal{I}_t(\underline{e}(m)))} \ln \frac{P_{Y_i|\mathcal{X}_{i-1:i}}(y_i|\underline{x}_{i-1:i}^*)}{P_{Y_i|\mathcal{X}_{i-1:i}}(y_i|\underline{x}(m)_{i-1:i})} \\ & \quad + \sum_{i \notin \mathcal{B}(m)} \ln \frac{P_{Y_i|\mathcal{X}_{i-1:i}}(y_i|\underline{x}_{i-1:i}^*)}{P_{Y_i|\mathcal{X}_{i-1:i}}(y_i|\underline{x}_{i-1:i}^*)} \\ &= \sum_{i=1}^N \ln \frac{P_{Y_i|\mathcal{X}_{i-1:i}}(y_i|\underline{x}_{i-1:i}^*)}{P_{Y_i|\mathcal{X}_{i-1:i}}(y_i|\underline{x}(m)_{i-1:i})} \\ &= \Lambda(\underline{x}^*, \underline{y}) - \Lambda(\underline{x}(m), \underline{y}), \end{aligned} \quad (15)$$

where we have used facts that $f_{\mathcal{I}(\underline{e}(m))}(\underline{x}^*) = \underline{x}(m)$ and $x_{i-1}(m) = x_{i-1}^*$, $x_i(m) = x_i^*$ if $i \notin \mathcal{B}(m)$.

Substituting (15) into (7), we have

$$\begin{aligned} \hat{m} &= \arg \min_{m=1, \dots, M} \sum_{t=1}^{\zeta(\mathcal{I}(\underline{e}(m)))} \gamma(\underline{y}, \mathcal{I}_t(\underline{e}(m))) \\ &= \arg \min_{m=1, \dots, M} \sum_{t=1}^{\zeta(\mathcal{I}(\underline{e}(m)))} \text{Rel}(\mathcal{I}_t(\underline{e}(m))) \\ &= \arg \min_{m=1, \dots, M} (\Lambda(\underline{x}^*, \underline{y}) - \Lambda(\underline{x}(m), \underline{y})) \\ &= \arg \max_{m=1, \dots, M} \Lambda(\underline{x}(m), \underline{y}) \\ &= m^*, \end{aligned} \quad (16)$$

thereby completing the proof.

B. Proof of Lemma 1

Based on the given conditions, we can write \mathcal{W} as

$$\mathcal{W} = \{\min(\mathcal{W}_1), \dots, \max(\mathcal{W}_1), \min(\mathcal{W}_2), \dots, \max(\mathcal{W}_2)\},$$

for which we have

$$\begin{aligned} & \text{Rel}(\mathcal{W}) \\ &= \Lambda(\underline{x}^*, \underline{y}) - \Lambda(f_{\mathcal{W}}(\underline{x}^*), \underline{y}) \\ &= \sum_{i=\min(\mathcal{W}_1)}^{\mathbf{R}_1(\mathcal{W}_2)} \ln \frac{P_{Y_i|\mathcal{X}_{i-1:i}}(y_i|\underline{x}_{i-1:i}^*)}{P_{Y_i|\mathcal{X}_{i-1:i}}(y_i|[f_{\mathcal{W}}(\underline{x}^*)]_{i-1:i})}. \end{aligned} \quad (17)$$

Given that $\min(\mathcal{W}_2) - \max(\mathcal{W}_1) > 1$, and noting that the following identities hold,

$$\begin{cases} [f_{\mathcal{W}}(\underline{x}^*)]_i = [f_{\mathcal{W}_1}(\underline{x}^*)]_i & \text{L}_1(\mathcal{W}_1) \leq i \leq \max(\mathcal{W}_1) + 1, \\ x_i^* = [f_{\mathcal{W}}(\underline{x}^*)]_i & \max(\mathcal{W}_1) + 1 \leq i \leq \min(\mathcal{W}_2) - 1, \\ [f_{\mathcal{W}}(\underline{x}^*)]_i = [f_{\mathcal{W}_2}(\underline{x}^*)]_i & \min(\mathcal{W}_2) - 1 \leq i \leq \text{R}_1(\mathcal{W}_2), \end{cases}$$

we can obtain

$$\begin{aligned} \text{Rel}(\mathcal{W}) &= \sum_{i=\min(\mathcal{W}_1)}^{\max(\mathcal{W}_1)+1} \ln \frac{P_{Y_i|\underline{X}_{i-1:i}}(y_i|\underline{x}_{i-1:i}^*)}{P_{Y_i|\underline{X}_{i-1:i}}(y_i|[f_{\mathcal{W}}(\underline{x}^*)]_{i-1:i})} \\ &+ \sum_{i=\max(\mathcal{W}_1)+2}^{\min(\mathcal{W}_2)-1} \ln \frac{P_{Y_i|\underline{X}_{i-1:i}}(y_i|\underline{x}_{i-1:i}^*)}{P_{Y_i|\underline{X}_{i-1:i}}(y_i|[f_{\mathcal{W}}(\underline{x}^*)]_{i-1:i})} \\ &+ \sum_{i=\min(\mathcal{W}_2)}^{\text{R}_1(\mathcal{W}_2)} \ln \frac{P_{Y_i|\underline{X}_{i-1:i}}(y_i|\underline{x}_{i-1:i}^*)}{P_{Y_i|\underline{X}_{i-1:i}}(y_i|[f_{\mathcal{W}}(\underline{x}^*)]_{i-1:i})} \\ &= \text{Rel}(\mathcal{W}_1) + \text{Rel}(\mathcal{W}_2). \end{aligned} \quad (18)$$

This completes the proof.

C. Proof of Lemma 2

For each sum term on the right-hand side of (9), after some algebraic manipulations, we obtain

$$\begin{aligned} &\text{Rel}(\{i, i+1\}) - \text{Rel}(\{i\}) - \text{Rel}(\{i+1\}) \\ &= \ln \frac{P_{Y_{i+1}|\underline{X}_{i:i+1}}(y_{i+1}|x_i^*, x_{i+1}^* \oplus 1)}{P_{Y_{i+1}|\underline{X}_{i:i+1}}(y_{i+1}|x_i^*, x_{i+1}^*)} \\ &+ \ln \frac{P_{Y_{i+1}|\underline{X}_{i:i+1}}(y_{i+1}|x_i^* \oplus 1, x_{i+1}^*)}{P_{Y_{i+1}|\underline{X}_{i:i+1}}(y_{i+1}|x_i^* \oplus 1, x_{i+1}^* \oplus 1)}. \end{aligned}$$

On the other hand, the left-hand side of (9) can be written as

$$\begin{aligned} &\text{Rel}(\mathcal{W}) - \left(\text{Rel}(\{a\}) + \dots + \text{Rel}(\{a + |\mathcal{W}| - 1\}) \right) \\ &= \sum_{i=a+1}^{a+|\mathcal{W}|-1} \ln \frac{P_{Y_i|\underline{X}_{i-1:i}}(y_i|x_{i-1}^*, x_i^* \oplus 1)}{P_{Y_i|\underline{X}_{i-1:i}}(y_i|x_{i-1}^*, x_i^*)} \\ &+ \sum_{i=a+1}^{a+|\mathcal{W}|-1} \ln \frac{P_{Y_i|\underline{X}_{i-1:i}}(y_i|x_{i-1}^* \oplus 1, x_i^*)}{P_{Y_i|\underline{X}_{i-1:i}}(y_i|x_{i-1}^* \oplus 1, x_i^* \oplus 1)} \\ &= \sum_{i=a}^{a+|\mathcal{W}|-2} \left(\text{Rel}(\{i, i+1\}) - \text{Rel}(\{i\}) - \text{Rel}(\{i+1\}) \right). \end{aligned} \quad (19)$$

This completes the proof.

D. Proof of Lemma 3

Define

$$\delta_i \triangleq \ln \frac{P_{Y_{i+1}|\underline{X}_{i:i+1}}(y_{i+1}|1, 1)}{P_{Y_{i+1}|\underline{X}_{i:i+1}}(y_{i+1}|0, 1)} + \ln \frac{P_{Y_{i+1}|\underline{X}_{i:i+1}}(y_{i+1}|0, 0)}{P_{Y_{i+1}|\underline{X}_{i:i+1}}(y_{i+1}|1, 0)}. \quad (20)$$

Then, it follows that

$$\begin{aligned} \delta_i &= \frac{1}{2\sigma^2} \left(- \left(y_{i+1} - (h_0 + h_1) \right)^2 - \left(y_{i+1} + (h_0 + h_1) \right)^2 \right. \\ &\quad \left. + \left(y_{i+1} - (h_1 - h_0) \right)^2 + \left(y_{i+1} - (h_0 - h_1) \right)^2 \right) \\ &= \frac{-4h_0h_1}{\sigma^2}, \end{aligned} \quad (21)$$

where we have used the fact that BPSK modulation maps bit 0 to +1 and bit 1 to -1. Therefore, we obtain

$$\begin{aligned} &\text{Rel}(\{i, i+1\}) - \text{Rel}(\{i\}) - \text{Rel}(\{i+1\}) \\ &= \frac{4h_0h_1}{\sigma^2} [2 \times \mathbf{1}(x_i^* = x_{i+1}^*) - 1]. \end{aligned} \quad (22)$$

E. Proof of Lemma 4

Based on Definition 2, we have

$$\text{Rel}(\mathcal{W}) = \sum_{i=\min(\mathcal{W}_1)}^{\text{R}_L(\mathcal{W}_2)} \ln \frac{P_{Y_i|\underline{X}_{i-L:i}}(y_i|\underline{x}_{i-L:i}^*)}{P_{Y_i|\underline{X}_{i-L:i}}(y_i|[f_{\mathcal{W}}(\underline{x}^*)]_{i-L:i})}. \quad (23)$$

Since $\min(\mathcal{W}_2) - \max(\mathcal{W}_1) > L$, the above summation can be decomposed into three parts. Moreover, using the following identities,

$$\begin{cases} [f_{\mathcal{W}}(\underline{x}^*)]_i = [f_{\mathcal{W}_1}(\underline{x}^*)]_i, & \text{L}_L(\mathcal{W}_1) \leq i \leq \max(\mathcal{W}_1) + L, \\ [f_{\mathcal{W}}(\underline{x}^*)]_i = x_i^*, & \max(\mathcal{W}_1) + 1 \leq i \leq \min(\mathcal{W}_2) - 1, \\ [f_{\mathcal{W}}(\underline{x}^*)]_i = [f_{\mathcal{W}_2}(\underline{x}^*)]_i, & \min(\mathcal{W}_2) - L \leq i \leq \text{R}_L(\mathcal{W}_2), \end{cases}$$

the remainder of the proof follows in the same manner as that of Lemma 1 in Appendix VII-B.

F. Proof of Lemma 5

First, consider the case where $\max(\mathcal{W}_1) + L < N$. We have

$$\begin{aligned} \text{Rel}(\mathcal{W}) &= \sum_{i=\min(\mathcal{W}_1)}^{\min(\mathcal{W}_2)-1} \ln \frac{P_{Y_i|\underline{X}_{i-L:i}}(y_i|\underline{x}_{i-L:i}^*)}{P_{Y_i|\underline{X}_{i-L:i}}(y_i|[f_{\mathcal{W}}(\underline{x}^*)]_{i-L:i})} \\ &+ \sum_{i=\max(\mathcal{W}_1)+L+1}^{\text{R}_L(\mathcal{W}_2)} \ln \frac{P_{Y_i|\underline{X}_{i-L:i}}(y_i|\underline{x}_{i-L:i}^*)}{P_{Y_i|\underline{X}_{i-L:i}}(y_i|[f_{\mathcal{W}}(\underline{x}^*)]_{i-L:i})} \\ &+ \sum_{i=\min(\mathcal{W}_2)}^{\max(\mathcal{W}_1)+L} \ln \frac{P_{Y_i|\underline{X}_{i-L:i}}(y_i|\underline{x}_{i-L:i}^*)}{P_{Y_i|\underline{X}_{i-L:i}}(y_i|[f_{\mathcal{W}}(\underline{x}^*)]_{i-L:i})}. \end{aligned} \quad (24)$$

Under the condition that $2 \leq \min(\mathcal{W}_2) - \max(\mathcal{W}_1) \leq L$, using the identities

$$\begin{cases} [f_{\mathcal{W}}(\underline{x}^*)]_i = [f_{\mathcal{W}_1}(\underline{x}^*)]_i, & \text{L}_L(\mathcal{W}_1) \leq i \leq \min(\mathcal{W}_2) - 1, \\ [f_{\mathcal{W}}(\underline{x}^*)]_i = [f_{\mathcal{W}_2}(\underline{x}^*)]_i, & \max(\mathcal{W}_1) + L + 1 \leq i \leq \text{R}_L(\mathcal{W}_2), \end{cases}$$

and applying straightforward algebraic manipulations to the expressions of $\text{Rel}(\mathcal{W}_1)$ and $\text{Rel}(\mathcal{W}_2)$, we obtain (12).

Next, consider the case where $\max(\mathcal{W}_1) + L \geq N$. We have

$$\begin{aligned} & \text{Rel}(\mathcal{W}) \\ &= \sum_{i=\min(\mathcal{W}_1)}^{\min(\mathcal{W}_2)-1} \ln \frac{P_{Y_i|X_{i-L:i}}(y_i|x_{i-L:i}^*)}{P_{Y_i|X_{i-L:i}}(y_i|[f\mathcal{W}(\underline{x}^*)]_{i-L:i})} \\ &+ \sum_{i=\min(\mathcal{W}_2)}^N \ln \frac{P_{Y_i|X_{i-L:i}}(y_i|x_{i-L:i}^*)}{P_{Y_i|X_{i-L:i}}(y_i|[f\mathcal{W}(\underline{x}^*)]_{i-L:i})}. \end{aligned} \quad (25)$$

By similar algebraic manipulations, (12) also follows. This completes the proof.

REFERENCES

- [1] G. Durisi, T. Koch, and P. Popovski, "Toward massive, ultrareliable, and low-latency wireless communication with short packets," *Proc. IEEE*, vol. 104, no. 9, pp. 1711–1726, 2016.
- [2] H. Chen, R. Abbas, P. Cheng, M. Shirvanimoghaddam, W. Hardjawana, W. Bao, Y. Li, and B. Vucetic, "Ultra-reliable low latency cellular networks: Use cases, challenges and approaches," *IEEE Commun. Magazine*, vol. 56, no. 12, pp. 119–125, 2018.
- [3] K. R. Duffy, J. Li, and M. Médard, "Capacity-achieving guessing random additive noise decoding," *IEEE Trans. Inf. Theory*, vol. 65, no. 7, pp. 4023–4040, 2019.
- [4] W. An, M. Médard, and K. R. Duffy, "Keep the bursts and ditch the interleavers," *IEEE Trans. Commun.*, vol. 70, no. 6, pp. 3655–3667, 2022.
- [5] E. R. Berlekamp, "Algebraic coding theory," in *McGraw-Hill, New York*, 1968.
- [6] J. Massey, "Shift-register synthesis and BCH decoding," *IEEE Trans. Inf. Theory*, vol. 15, no. 1, pp. 122–127, 1969.
- [7] K. R. Duffy, M. Grundei, and M. Médard, "Using channel correlation to improve decoding-ORBGRAND-AI," in *Proc. IEEE Global Commun. Conf.*, 2023, pp. 3585–3590.
- [8] A. Viterbi, "Error bounds for convolutional codes and an asymptotically optimum decoding algorithm," *IEEE Trans. Inf. Theory*, vol. 13, no. 2, pp. 260–269, 1967.
- [9] M. Liu, Y. Wei, Z. Chen, and W. Zhang, "ORBGRAND is almost capacity-achieving," *IEEE Trans. Inf. Theory*, vol. 69, no. 5, pp. 2830–2840, 2022.
- [10] E. Biglieri, J. Proakis, and S. Shamai, "Fading channels: Information-theoretic and communications aspects," *IEEE Trans. Inf. Theory*, vol. 44, no. 6, pp. 2619–2692, 1998.
- [11] G. Forney and G. Ungerboeck, "Modulation and coding for linear Gaussian channels," *IEEE Trans. Inf. Theory*, vol. 44, no. 6, pp. 2384–2415, 1998.
- [12] P. A. Van Walree, "Propagation and scattering effects in underwater acoustic communication channels," *IEEE J. Ocean. Eng.*, vol. 38, no. 4, pp. 614–631, 2013.
- [13] B. Saleh and M. Irshid, "Coherence and intersymbol interference in digital fiber optic communication systems," *IEEE J. Quantum Electron.*, vol. 18, no. 6, pp. 944–951, 2003.
- [14] P. H. Siegel and J. K. Wolf, "Modulation and coding for information storage," *IEEE Commun. Magazine*, vol. 29, no. 12, pp. 68–86, 1991.
- [15] G. Forney, "Maximum-likelihood sequence estimation of digital sequences in the presence of intersymbol interference," *IEEE Trans. Inf. Theory*, vol. 18, no. 3, pp. 363–378, 1972.
- [16] R. Lucky, J. Salz, and E. Weldon, *Principles of Data Communication*. McGraw-Hill, 1968.
- [17] P. Mosen, "Feedback equalization for fading dispersive channels," *IEEE Trans. Inf. Theory*, vol. 17, no. 1, pp. 56–64, 1971.
- [18] C. A. Belfiore and J. H. Park, "Decision feedback equalization," *Proc. IEEE*, vol. 67, no. 8, pp. 1143–1156, 1979.
- [19] D. D. Falconer and F. Magee Jr, "Adaptive channel memory truncation for maximum likelihood sequence estimation," *Bell System Technical Journal*, vol. 52, no. 9, pp. 1541–1562, 1973.
- [20] S. Qureshi and E. Newhall, "Adaptive receiver for data transmission over time-dispersive channels," *IEEE Trans. Inf. Theory*, vol. 19, no. 4, pp. 448–457, 1973.
- [21] W. Lee and F. Hill, "A maximum-likelihood sequence estimator with decision-feedback equalization," *IEEE Trans. Commun.*, vol. 25, no. 9, pp. 971–979, 1977.
- [22] C. Beare, "The choice of the desired impulse response in combined linear-Viterbi algorithm equalizers," *IEEE Trans. Commun.*, vol. 26, no. 8, pp. 1301–1307, 1978.
- [23] C. Douillard, M. Jézéquel, C. Berrou, D. Electronique, A. Picart, P. Didier, and A. Glavieux, "Iterative correction of intersymbol interference: turbo-equalization," *Eur. Trans. Telecommun.*, vol. 6, no. 5, pp. 507–511, 1995.
- [24] K. R. Duffy, M. Médard, and W. An, "Guessing random additive noise decoding with symbol reliability information (SRGRAND)," *IEEE Trans. Commun.*, vol. 70, no. 1, pp. 3–18, 2021.
- [25] A. Solomon, K. R. Duffy, and M. Médard, "Soft maximum likelihood decoding using GRAND," in *Proc. IEEE Int. Conf. Commun. (ICC)*, 2020, pp. 1–6.
- [26] K. R. Duffy, W. An, and M. Médard, "Ordered reliability bits guessing random additive noise decoding," *IEEE Trans. Signal Process.*, vol. 70, pp. 4528–4542, 2022.
- [27] C. Condo, V. Bioglio, and I. Land, "High-performance low-complexity error pattern generation for ORBGRAND decoding," in *Proc. IEEE Globecom Workshops (GC Wkshps)*, 2021, pp. 1–6.
- [28] S. M. Abbas, T. Tonnellier, F. Ercan, M. Jaleddine, and W. J. Gross, "High-throughput and energy-efficient VLSI architecture for ordered reliability bits GRAND," *IEEE Trans. Very Large Scale Integr. (VLSI) Syst.*, vol. 30, no. 6, pp. 681–693, 2022.
- [29] C. Condo, "A fixed latency ORBGRAND decoder architecture with LUT-aided error-pattern scheduling," *IEEE Trans. Circuits and Sys. I: Reg. Papers*, vol. 69, no. 5, pp. 2203–2211, 2022.
- [30] Z. Li and W. Zhang, "ORBGRAND: Achievable rate for general bit channels and application in BICM," in *Proc. IEEE Int. Symp. Pers., Ind. Mobile Radio Commun.*, 2024, pp. 1–7.
- [31] Z. Li and W. Zhang, "ORBGRAND is exactly capacity-achieving via rank companding," 2025, [arXiv:2512.00347](https://arxiv.org/abs/2512.00347).
- [32] L. Wan, H. Yin, and W. Zhang, "A parallelization strategy for GRAND with optimality guarantee by exploiting error pattern tree representation," 2025, [arXiv:2510.01813](https://arxiv.org/abs/2510.01813).